Detection and Characterization of Alkyl Peroxy Radicals Using Cavity Ringdown Spectroscopy

Michael B. Pushkarsky, Sergey J. Zalyubovsky, and Terry A. Miller

Laser Spectroscopy Facility

Department of Chemistry

The Ohio State University

120 W. 18th Avenue

Columbus Ohio 43210

April 20, 2000

Abstract

Cavity ringdown spectra of the $\tilde{A}\ ^2\mathrm{A}'-\tilde{X}\ ^2\mathrm{A}''$ electronic transition in the IR are reported for the methyl and ethyl peroxy radicals. Analysis of partially resolved rotational structure for the origin band of the transition provides information about both the $\tilde{A}$ and $\tilde{X}$ states of $CH_3O_2\cdot$. An estimate for the absorption cross-section is determined from the CRDS absorption and the rate of radical-radical recombination.

Low temperature oxidation of hydrocarbons is a pervasive process in both nature and technology. It is critically important for the environmental quality of our atmosphere.[1–5] Similarly it is critical to the efficiency and fuel economy of internal combustion engines.[6–8] Arguably the most important reaction[7] for low temperature oxidation is the production of peroxy radicals ($RO_2\cdot$) from alkyl radicals ($R\cdot$), i.e., $R\cdot + O_2 + M \rightarrow RO_2\cdot + M$.

There are a number of important alkyl peroxy radicals defined by the nature of the R group, ranging

from the simplest species, methyl (R=CH_3) peroxy to complex species with R containing at least 8-10 carbon atoms with correspondingly many structural isomers. Because of their significance, much effort[1] has been expended studying the mechanisms and kinetics of peroxy radical production and their subsequent reactions. This work has largely been based upon monitoring of the peroxy radicals via their $\tilde{B}^2\mathrm{A}'' - \tilde{\mathrm{X}}^2\mathrm{A}''$ UV absorption. This is a strong transition, common to all the peroxies, that is centered around 240nm. Unfortunately this transition is broad and unstructured with a half-width of ≈40nm. The quasi-continuum nature of this transition has at least two clear disadvantages. It is unsuitable for obtaining rotational or vibrational information about the radical. Additionally the overlapping of the UV spectra of different $RO_2\cdot$ radicals makes the identification of a specific alkyl peroxy radical, particularly from a mixture, a significant challenge.

Experiments involving the peroxy $\tilde{A}^2\mathrm{A}' - \tilde{X}^2\mathrm{A}''$ transition in the IR are sparse. There was an early report,[9] using low resolution modulated absorption spectroscopy, of the observation of the $\tilde{A}-\tilde{X}$ IR transition of several $RO_2\cdot$ radicals and more recently a report[10] of the observation of fragmentary spectra of ethyl peroxy using a cw absorption technique. There was also a report[11] of the detection of the $\tilde{A}-\tilde{X}$ transition of $CH_3O_2\cdot$ by intracavity laser absorption spectroscopy, but few spectroscopic details were given. Based upon the recent observation[12] and analysis[13] of a well resolved spectrum of the hydroperoxy radical, $HO_2\cdot$, we expect the $\tilde{A}-\tilde{X}$ IR transitions of the alkyl peroxy radicals to be well structured and observable using cavity ringdown spectroscopy (CRDS).

Historically this IR transition has been viewed as difficult to study because of its small oscillator strength (the cross-section σ is $\approx 2\times10^{-21}$ cm^{-2} for the corresponding transition[13] in $HO_2\cdot$) and the near IR spectral region ($\approx 7000-8000$ cm^{-1}) in which the transition is located. However CRDS is a powerful technique[14–16] for dealing with these difficulties. The expected sharp IR transitions should yield resolved vibrational and rotational structure to characterize the peroxy radicals. Additionally, the $\tilde{A}-\tilde{X}$ spectra should easily distinguish between different $RO_2\cdot$ radicals even in a mixture. Finally the transient nature of CRDS experiments are readily adaptable for rapidly monitoring $RO_2\cdot$ concentrations and measuring the reaction kinetics of the radicals.

In this Communication, we report the initial observations of CRDS spectra for the methyl ($CH_3O_2\cdot$) and

ethyl ($C_2H_5O_2\cdot$) peroxy radicals and their per-deutero analogues. These results demonstrate the ability of CRDS to sensitively detect the $\tilde{A} - \tilde{X}$ IR transition, and the spectra show the expected sharp and resolvable vibrational and rotational structure. A preliminary analysis of the rotational structure of $CH_3O_2\cdot$ provides improved rotational constants compared to those available from high level *ab initio* calculations. Finally we have demonstrated the easy adaptability of our technique to the measurement of the reaction kinetics of $RO_2\cdot$ radicals.

In our experiments the required IR radiation near 1.3μm was generated by stimulated Raman shifting of the output of a dye laser in molecular hydrogen. The Nd:YAG pumped dye laser system was operated with LDS867 and LDS821 laser dyes, producing 15-30mJ/pulse of tunable radiation in the region of 820-880nm with a linewidth of $\approx$0.3 cm^{-1}. The output of the dye laser was focused by a 50cm focal length lens into a 70cm long, single-pass Raman cell, filled with 200-300psi of H_2. The first Stokes emission of 1-3mJ/pulse was collimated and weakly focussed into the reaction flow cell. Fundamental and anti-Stokes frequencies were suppressed using a color filter. The parallelopiped flow cell was fabricated of stainless steel and consists of a central part with two rectangular UV grade quartz photolysis windows (2cm$\times$18cm) and two 15cm-long arms on its ends where the cavity ring-down mirrors (Los Gatos Research) are mounted.

The IR radiation that passes through the cavity is focused onto an amplified InGaAs photodiode, with the transient signal being recorded by a digital oscilloscope. Typically 16 waveforms were averaged, the sum transferred to a computer and fit to a single exponential decay. The decay constant was converted to the relative absorption per pass (in ppm) and saved as a point in the spectrum. With empty cavity losses of 35 ppm per pass at the center of the mirror region, the sensitivity of the method is estimated as $\lesssim$1ppm absorption per pass.

The photolysis excimer laser (LPX300, Lambda Physik) was operated either at 248 nm (200mj/pulse) to photolyze iodoalkanes, or at 193 nm (150mJ/pulse) to photolyze ketones. The photolysis beam was shaped by cylindrical and spherical lenses to a rectangle, 16cm by 0.5 cm, and sent into the central part of flow cell, thereby determining the volume wherein radicals are created.

The photolysis pulse is fired approximately 100 μs before the dye laser, allowing time for peroxy radicals to be formed, but not enough time for them to recombine. Background subtraction was implemented to

eliminate absorption from the precursors and/or residual water, both of which have vibrational overtone and combination bands in the region of interest. With the probe laser fixed at a given frequency, the ring-down decay is recorded once after the photolysis laser fires and again with the photolysis laser off. This technique is effective in eliminating both broad features, e.g., absorptions of acetone, and sharp rotationally resolved lines of water. Background substraction is useful for "cleaning up" the spectrum for the rotational analysis described below. However the strong peroxy peaks are clearly visible in the spectrum even without background substraction.

In our initial experiments, we filled the cell with a mixture of 200 torr Ne and 50 torr O_2 plus 1-10 torr of a precursor for either the methyl radical (methyl iodide or acetone or perdeuterated isotopomers) or ethyl radical (iodoethane or 3-pentanone or perdeuterated isotopomers). In Fig. 1 we show a relatively broad spectral scan with two traces illustrating absorptions assigned to methyl peroxy and ethyl peroxy radicals.

For trace A of Figure 1, acetone was photolyzed, and the lower frequency band therein is attributed to the O–O band of the $\tilde{A}^2\mathrm{A}' - \tilde{\mathrm{X}}^2\mathrm{A}''$ transition of methyl peroxy. The weaker transition to higher frequency is attributed to a transition involving the methyl torsion in the radical. For trace B of Figure 1, 3-pentanone was photolyzed and the strong, higher frequency feature is assigned to the origin of the $\tilde{A}^2\mathrm{A}' - \tilde{\mathrm{X}}^2\mathrm{A}''$ transition in ethyl peroxy radical. At lower frequency we see a second, weaker absorption which we assign in part to $CH_3O_2\cdot$ due to its close resemblance to the origin band shown in trace A. The source of $CH_3O_2\cdot$ in trace B is not well determined, but the simplest explanation is that it is produced as a by-product of the reaction yielding mainly $C_2H_5O_2\cdot$, with the most probable source of the by-product arising from production of methyl radical in the initial photolysis step. In any case trace B demonstrates the importance of having a spectroscopic technique that is capable of distinguishing between the various alkyl peroxy radicals.

Fig. 2 shows on an expanded scale a portion of the $CD_3O_2\cdot$ spectrum. The experimental trace (A) clearly shows rotational structure. Unfortunately this structure is not completely resolved so that a line-by-line rotational assignment and analysis cannot be performed. It is well known that the analyses of rotational contours can provide rather detailed information about the rotational constants and ultimately the geometric structure of molecules. However a danger of such analyses lies in their lack of uniqueness. On occasion a contour analysis will produce a set of constants that will reproduce the spectrum, but are

actually quite different from a second, correct set that also reproduces the spectrum well. To minimize this problem we have determined rotational constants for both the $\tilde{X}$ and $\tilde{A}$ states of the methyl peroxy radical using ROHF/6-31+G(d) *ab initio* calculations via Gaussian98.

We have shown in trace C of Fig. 2 a simulation of the observed $\tilde{A} - \tilde{X}$ rotational structure generated by our SpecSim spectral analysis program using the *ab initio* rotational constants and neglecting any spin-rotation effects due to the doublet nature of the electronic state. As traces A and C of Fig. 2 show, there is a good qualitative resemblance between the experimental spectrum and that predicted by the *ab initio* constants. However there are also clear discrepancies between the two. We are then in a position to refine the *ab initio* rotational constants of both the $\tilde{A}$ and $\tilde{X}$ states to match the experimental spectrum. As shown in Fig. 2, traces A and B (simulated with the refined constants) are effectively indistinguishable within experimental variation.

The values of the experimentally fit and *ab initio* rotational constants used in Fig. 2 for $CD_3O_2\cdot$ are (in cm^{-1}): $A'' = 1.296(1.338)$, $B'' = 0.332(0.328)$ and $C'' = 0.290(0.293)$ with $A' = 1.182(1.249)$, $B' = 0.340(0.331)$ and $C' = 0.288(0.291)$ (*ab initio* values in parenthesis). The corresponding values for $CH_3O_2\cdot$ are $A'' = 1.716(1.799)$, $B'' = 0.384(0.390)$ and $C'' = 0.348(0.341)$ with $A' = 1.528(1.637)$, $B' = 0.391(0.392)$ and $C' = 0.345(0.337)$. As with the *ab initio* values no error limits are indicated for the experimental values. Notwithstanding the fact that we have gone to considerable effort to insure the "unique correctness" of our refined rotational constants, there is no absolute proof that these values represent the *only* set of rotational constants that reproduce the spectrum. However, probably more to the point the correlation among the constants, and the effects of neglecting spin-rotation interactions, are difficult to estimate. For the same reasons we do not pursue the geometric implications of these constants. However we expect soon (see below) to have completely resolved rotational spectra that will unambiguously resolve these issues. We have a high degree of confidence that our present experimental rotational constants will prove an excellent starting point for the analysis of the fully resolved spectrum. Finally from the rotational analyses come accurate values for T_{00} for $CH_3O_2\cdot$ and $CD_3O_2\cdot$ which are respectively 7382.8 ± 0.5 and 7372.6 ± 0.5 cm^{-1}. These values are in good agreement with the work of Hunziker and Wendt,[9] but of much higher precision.

Besides our initial spectroscopic results, we have performed one experiment that demonstrates the poten-

tial of CRDS for monitoring the reactions of peroxy radicals. We have set our laser frequency at the origin of the $CH_3O_2\cdot$ $\tilde{A}^2A' - \tilde{X}^2A''$ electronic transition. We then measure the decay of the absorption as a function of time after the $CH_3O_2\cdot$ is produced by the photolysis of acetone by the excimer laser. This decay should be due almost entirely to radical-radical recombination. Defining the observed rate constant, k_{obs}, by

$$\frac{d[CH_3O_2\cdot]}{dt} = -2k_{obs}[CH_302\cdot]^2 \tag{1}$$

and integrating yields

$$\frac{[CH_3O_2\cdot]_0}{[CH_3O_2\cdot]} = 1 + 2k_{obs}[CH_302\cdot]_0 t \tag{2}$$

The experimental results are plotted in this form in Fig. 3, which shows a good straight line as expected. From the slope, $2k_{obs}[CH_3O_2\cdot]_0$, and the known[1] value of $k_{obs} = 4.9 \times 10^{-13}$ cm^3 s^{-1}, we obtain the initial concentration, $[CH_3O_2\cdot]_0$. Combination of $[CH_3O_2\cdot]_0$ with our absolute absorption measurements (see, for example, Fig. 1) yields an empirical peak absorption cross-section $\sigma \approx 2.7 \times 10^{-20}$ cm^2 for the origin under our experimental conditions. While the precision of our experiments is considerably better, we estimate the overall error in σ is $\lesssim$50%, considering possible systematic errors such as inhomogenities in radical production in the cell, etc. We believe that additional experiments with a somewhat re-designed apparatus can significantly reduce these errors. There is always the possibility of other systematic errors, e.g., other radical reactions or peroxy radical diffusion out of the observation region. We have considered these possibilities in some detail and conclude that they either make minor contributions or are ruled out completely by the time scale and the concentration dependence of the plots of Fig. 3.

The value for σ is about an order of magnitude greater than that expected for the strongest rotational transition of $CH_3O_2\cdot$ assuming the same oscillator as reported for $HO_2\cdot$. However the observed σ is very consistent with our rotational simulations which indicate that the strong peak in the 0–0 band corresponds to the supersurposition of 10-20 rotational transitions. While σ is rather small for an allowed electronic transition, the fact that it is about an order of magnitude larger than might have been anticipated is encouraging for the use of CRDS spectroscopy to monitor peroxy radical reactions in applications relevant

to both atmospheric and combustion related hydrocarbon oxidation.

We believe that the present experiments demonstrate the potential for exploring the IR spectra of the $RO_2\cdot$ peroxy radicals with CRDS. In future experiments we plan to attempt to observe the spectra of many other peroxy radicals with small to moderate alkyl groups, halogenated alkyl groups, and other groups such as allyl, acetyl, phenyl, etc. In many cases, we expect to obtain fully resolved rotational spectra by using our high resolution pulse amplified laser system[17,18] with a fundamental resolution of ≈100 MHz. With this laser system we can also probe peroxy radicals produced in a supersonic free jet expansion so that detailed rotational analyses of even moderately large radicals will be possible. Finally we plan to further explore the capability of CRDS spectroscopy to measure concentrations and reaction kinetics of individual $RO_2\cdot$ radicals contained in complex gas mixtures.

Acknowledgement: The authors gratefully acknowledge Brian Applegate's help in producing the *ab initio* calculations and the financial support of this work by the National Science Foundation via grant CHE-9974404. We also acknowledge a grant of computer time from the Ohio Supercomputer Center.

References

[1] P. D. Lightfoot, R. A. Cox, J. N. Crowley, M. Destriau, G. D. Hayman, M. E. Jenkin, G. K. Moortgat, and F. Zabel, Atmos. Envir. **26A**, 1805 (1992).

[2] T. J. Wallington, P. Dagaut, and M. J. Kurylo, Chem. Rev. **92**, 667 (1992).

[3] E. P. Clifford, P. G. Wenthold, R. Gareyev, W. C. Lineberger, C. H. DePuy, V. M. Bierbaum, and G. B. Ellison, J. Chem. Phys. **109**, 10293 (1998).

[4] G. J. Frost, G. B. Ellison, and V. Vaida, J. Phys. Chem. A **103**, 10169 (1999).

[5] B. J. Finlayson-Pitts and J. J. N. Pitts, Science **276**, 1045 (1997).

[6] S. Wang, D. L. Miller, N. P. Cernansky, H. J. Curran, W. J. Pitz, and C. K. Westbrook, Combustion and Flame **118**, 415 (1999).

[7] H. J. Curran, P. Gaffuri, W. J. Pitz, and C. K. Westbrook, Combustion and Flame **114**, 149 (1998).

[8] C. K. Westbrook, W. J. Pitz, and W. R. Leppard, *SAE Technical Paper Series* (International Fuels and Lubricants Meeting and Exposition, Toronto, Canada, October 7-10, 1991).

[9] H. E. Hunziker and H. R. Wendt, J. Chem. Phys. **64**, 3488 (1976).

[10] D. B. Atkinson, *Book of Abstracts for 25th International Symposium on Free Radicals* (Flagstaff, AZ, 1999), p. 31.

[11] V. P. Bulatov, Y. V. Matyagin, O. M. Sarkisov, and E. A. Sviridenkov, Khim. Fiz. **10**, 311 (1991).

[12] E. H. Fink and D. A. Ramsay, J. Mol. Spec. **185**, 304 (1997).

[13] G. Osmann, P. R. Bunker, P. Jensen, R. J. Buenker, J. Gu, and G. Hirsch, J. Mol. Spectros. **197**, 262 (1999).

[14] J. J. Scherer, J. B. Paul, A. O'Keefe, and R. J. Saykally, Chem. Rev. **97**, 25 (1997).

[15] P. Zalicki and R. N. Zare, J. Chem. Phys. **102**, 2708 (1995).

[16] D. Romanini and K. K. Lehmann, J. Chem. Phys. **99**, 6287 (1993).

[17] R. R. Wright and T. A. Miller, J. Mol. Spectros. **194**, 219 (1999).

[18] C. C. Carter, T. A. Miller, H.-S. Lee, A. B. McCoy, and E. F. Hayes, J. Chem. Phys. **110**, 5065 (1999).

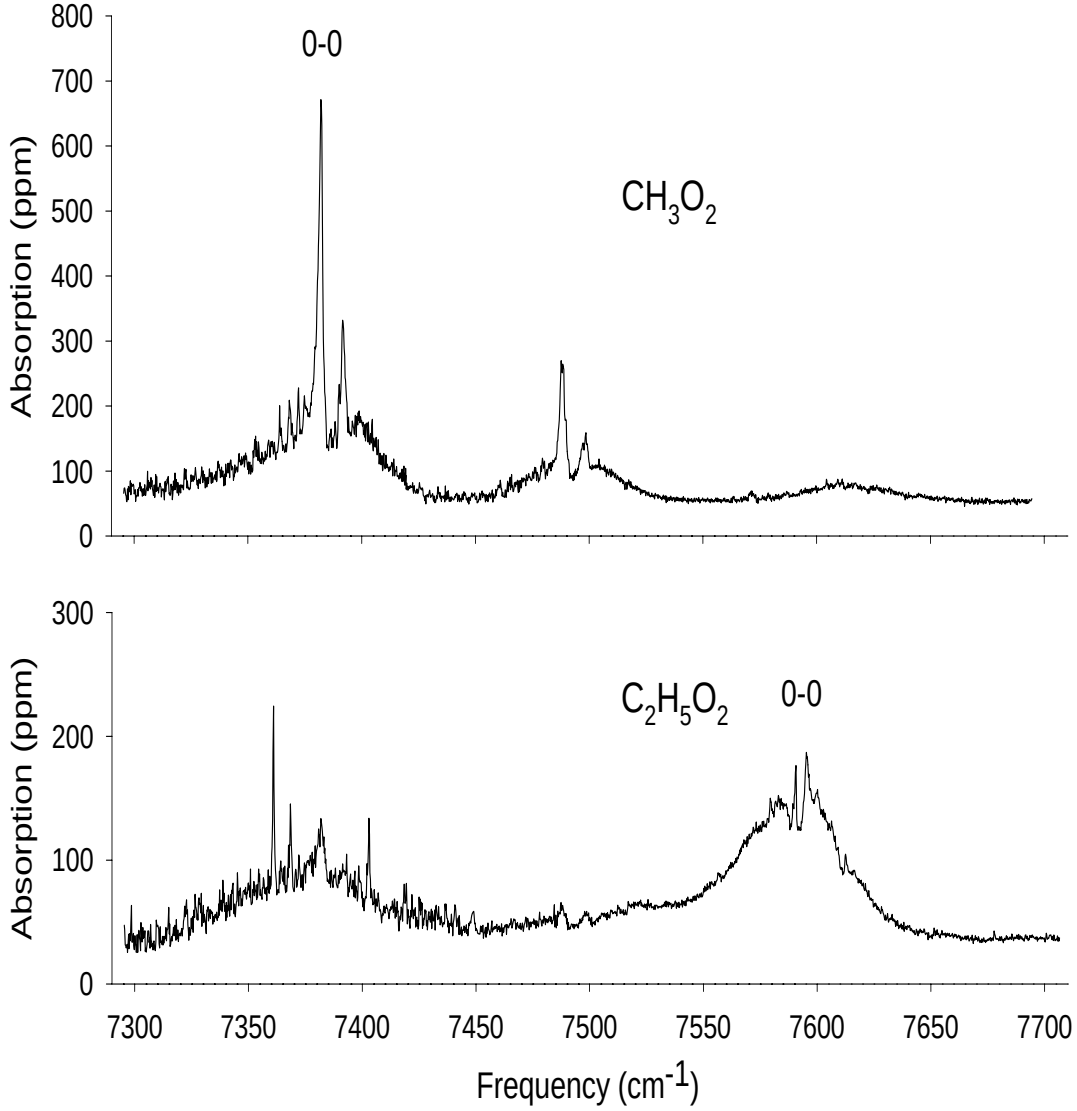

Figure 1: Experimental CRDS spectra following photolysis of acetone (top) and 3-pentanone (bottom). In the top trace the origin band of methyl peroxy radical is indicated; the feature to higher frequency likely arises from a "hot" methyl torsional transition. In the bottom trace the origin of the ethyl peroxy radical is indicated. At the low frequency end of this trace there are several weaker absorptions that have been determined experimentally to arise from the reaction of the photolysis products of 3-pentanone with O_2. Almost certainly part of these absorptions is due to $CH_3O_2\cdot$ but there appears as well to be other lines not attributable to $CH_3O_2\cdot$.

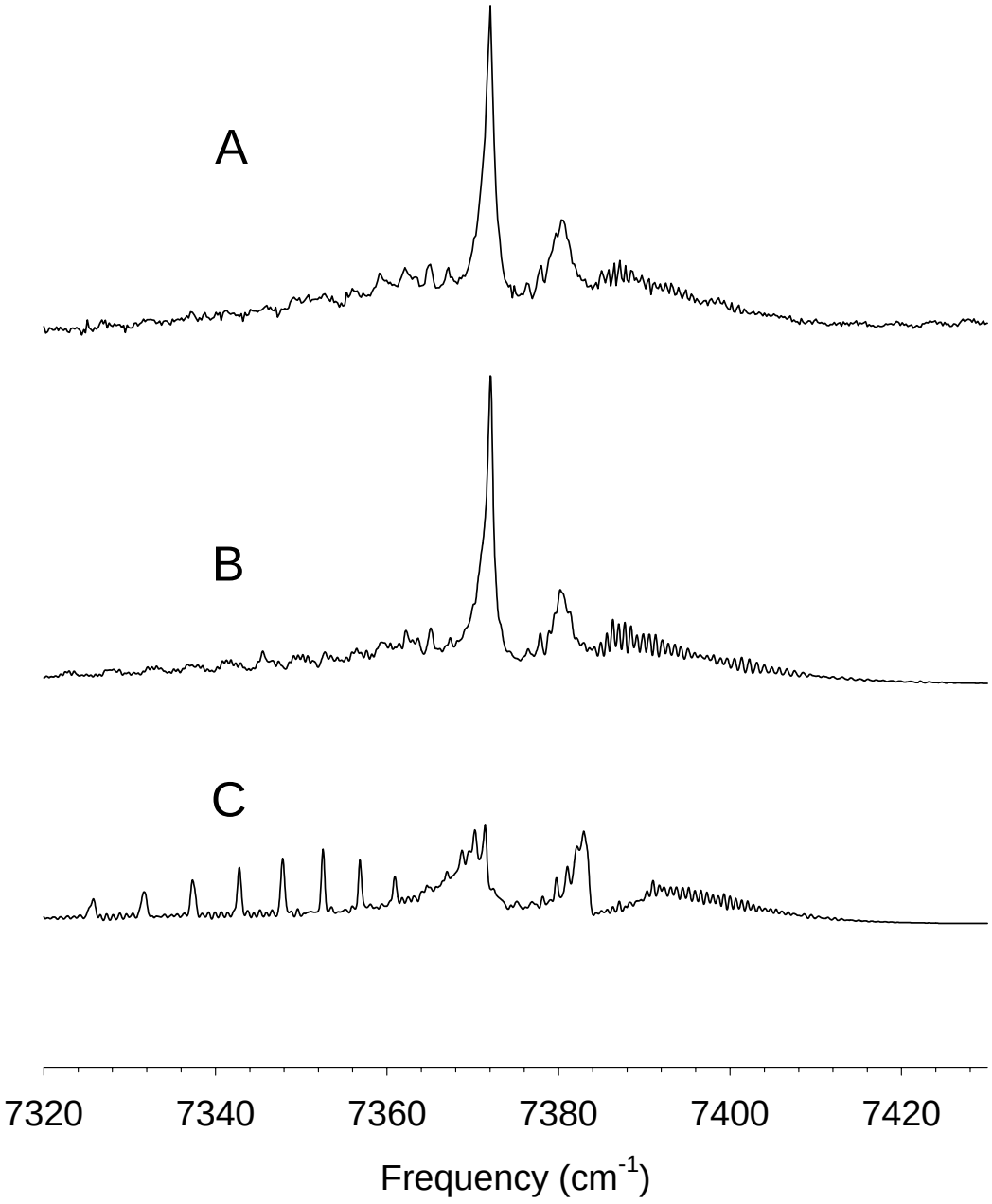

Figure 2: Spectra of CD_3O_2· radical from (A) the CRDS experiment, (C) a simulation using the *ab initio* rotational constants, and (B) a simulation designed to best reproduce the experimental spectrum by refining the *ab initio* rotational constants to best fit values. The best fit and the *ab initio* values used are given in the text for both CD_3O_2 and CH_3O_2.

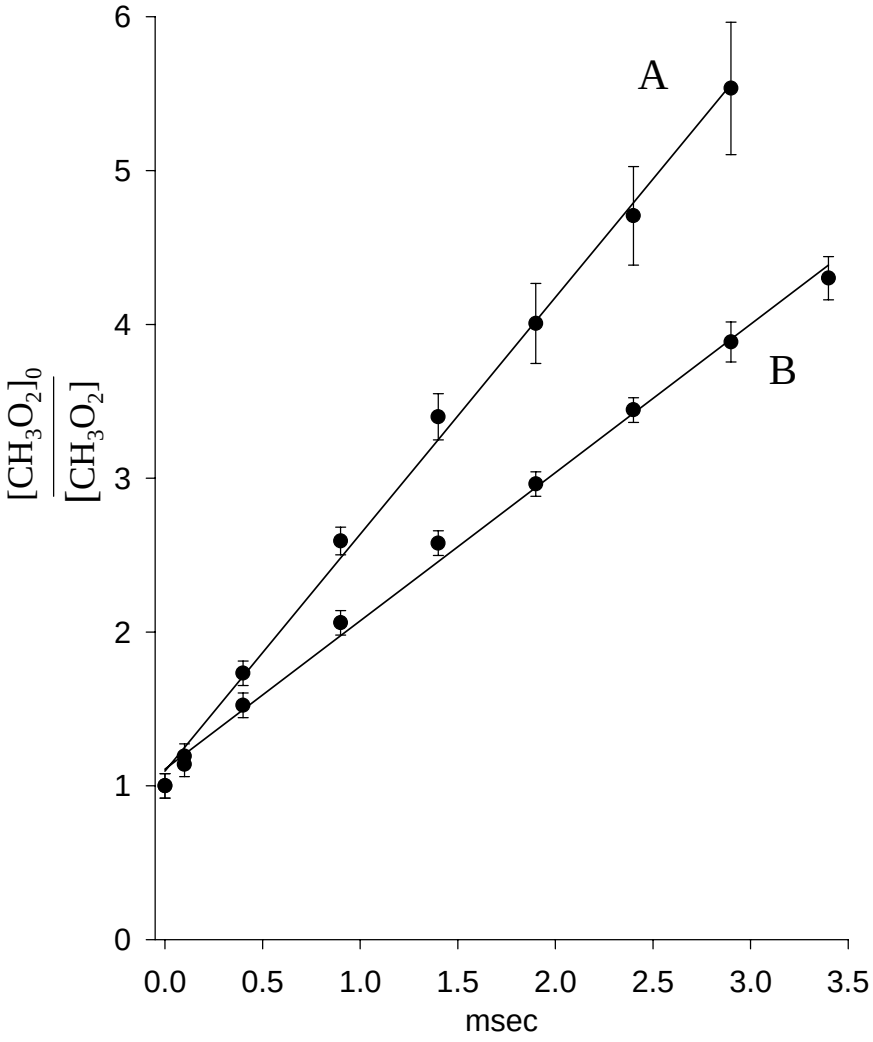

Figure 3: Methyl peroxy radical decay plots of the form of Eq. 2. Relative concentrations of $CH_3O_2\cdot$ are determined by the ratio of absorption at various times to that at $t = 0$. Plot (A) corresponds to an initial, net absorption of 515 ppm and (B) to 349 ppm.